Impact of molecular weight on charge carrier dissociation in solar cells from a polyfluorene derivative

Moet, D. J. D.; Lenes, M.; Kotlarski, J. D.; Veenstra, S. C.; Sweelssen, J.; Koetse, M. M.; de Boer, B.; Blom, P. W. M.

Published in:
Organic Electronics

DOI:
10.1016/j.orgel.2009.07.002

Publication date:
2009

Organic Electronics 10 (2009) 1275–1281

Contents lists available at ScienceDirect

Organic Electronics

journal homepage: www.elsevier.com/locate/orgel

Impact of molecular weight on charge carrier dissociation in solar cells from a polyfluorene derivative

D.J.D. Moet [a,*], M. Lenes [a,d], J.D. Kotlarski [a], S.C. Veenstra [b,d], J. Sweelssen [c,d], M.M. Koetse [c,d], B. de Boer [a,1], P.W.M. Blom [a,c]

[a] Zernike Institute for Advanced Materials, University of Groningen, Nijenborgh 4, 9747 AG Groningen, The Netherlands
[b] Energy Research Centre of the Netherlands (ECN), P.O. Box 1, 1755 ZG Petten, The Netherlands
[c] Holst Centre/TNO, High Tech Campus 31, 5605 KN Eindhoven, The Netherlands
[d] Dutch Polymer Institute, P.O. Box 902, 5600 AX Eindhoven, The Netherlands

ARTICLE INFO

Article history:
Received 5 June 2009
Received in revised form 1 July 2009
Accepted 3 July 2009
Available online 9 July 2009

PACS:
84.60.Jt
82.35.Cd
87.15.Ht

Keywords:
Polymer
Solar cells
Molecular weight
Dissociation
Polyfluorene

ABSTRACT

The effect of the molecular weight of poly[9,9-didecanefluorene-alt-(bis-thienylene) benzothiadiazole] (PF10TBT) on the photovoltaic performance of fullerene-based bulk heterojunction solar cells is investigated. An increase in molecular weight of two orders of magnitude results in a 30% increase of the short-circuit current and a rise of the fill factor from 0.45 to 0.63. Electron and hole transport are found to be virtually unaffected by changing molecular weight, which means that space-charge effects do not play a role in low molecular weight devices. Using optical modeling and numerical device simulations, we demonstrate that at low molecular weight the efficiency is mainly limited by a short lifetime of bound electron–hole pairs. This short lifetime prohibits efficient dissociation and is attributed to a deficiency in phase separation for low molecular weights.

1. Introduction

The field of polymer photovoltaics has made tremendous progress in terms of performance since the introduction of the bulk heterojunction concept [1]. This approach employs nanometer-scale intermixing of electron donating and accepting materials to enhance their interfacial area, thereby facilitating ultrafast electron transfer from the photoexcited polymer to an acceptor molecule. If there is sufficient phase separation, charge transfer can be followed by efficient dissociation of resulting bound electron–hole pairs and subsequent transport of free charge carriers to the electrodes. Systems of conjugated polymers as donor (D) and soluble C_{60} derivatives as acceptor (A) currently bear the largest potential for energy conversion with state-of-the-art confirmed efficiencies approaching 6% [2].

Polyfluorene copolymers have shown to be suitable candidates for efficient solar cells [3–5]. A promising power conversion efficiency of 4.2% has been reported for a system of poly[9,9-didecanefluorene-alt-(bis-thienylene) benzothiadiazole] (PF10TBT) and [6,6]-phenyl C_{61}-butyric acid methyl ester (PCBM) [6]. By virtue of the polymer's highest occupied molecular orbital (HOMO) energy level at 5.4 eV, PF10TBT:PCBM solar cells deliver outstanding

* Corresponding author.
E-mail addresses: d.j.d.moet@rug.nl, date.moet@gmail.com (D.J.D. Moet).
[1] Deceased 27 January 2009.

1566-1199/$ - see front matter © 2009 Elsevier B.V. All rights reserved.
doi:10.1016/j.orgel.2009.07.002

open-circuit voltages of around 1 V. Moreover, in contrast to many other conjugated polymers, the lowest unoccupied molecular orbital (LUMO) energy level at 3.4 eV is close in energy to that of PCBM. Therefore, less voltage is lost during electron transfer at the D–A interface [7]. However, the photovoltaic performance of PF10TBT cells is strongly dependent on the molecular weight (MW) of the polymer [8]. Low MW devices show significantly lower short-circuit currents and fill factors, resulting in a reduction of the maximum output power by a factor of 2 compared to the best high MW devices.

For the further design of new donor polymers understanding of the dependence of solar cell performance on their chemical and structural properties is crucial. Low fill factors are commonly attributed to unbalanced charge carrier transport in the polymer and fullerene phase [9]. Molecular weight dependent hole mobilities have been observed in regioregular poly(3-hexylthiophene) (P3HT), using field-effect transistor measurements [10–12], space-charge limited currents [13] and the time-of-flight technique [14]. Most studies revealed an increase of the hole mobility with increasing molecular weight. Suggested causes include differences in chain packing, interconnectivity of the polymer network, backbone conformation and interchain hopping. It has been pointed out by Goodman and Rose that in a solar cell with a significant difference in the hole- and electron mean free path, accumulation of the slowest charge carriers will lead to a nonuniform electric field in the device [15]. When the slowest carrier has a very low mobility the photocurrent can even reach a maximum electrostatically allowed limit at high light intensity [9]. This space-charge limited (SCL) photocurrent has a three quarter power dependence on light intensity and a square root dependence on voltage, which limits the fill factor to 0.42.

A different cause of a low fill factor was recently identified in solar cells from a narrow band gap polymer and PCBM [16]. The low fill factor again results from a square root dependence of the photocurrent on voltage, albeit for entirely different physical reasons than in the space-charge limited case. Here, the photocurrent is limited by a small product of mobility and lifetime of free charge carriers due to recombination or trapping and is described by [15]:

$$J_{\mathrm{ph}} = qG(\mu_{h(e)}\tau_{h(e)})^{1/2}V^{1/2} \quad (1)$$

where G is the generation rate of free charge carriers and $\mu_{h(e)}$ and $\tau_{h(e)}$ are the mobility and lifetime of free holes (electrons), respectively. Experimentally, this recombination limited photocurrent can be discriminated from the SCL case since it depends linearly on light intensity. Furthermore, the saturation voltage V_{sat}, at which the photocurrent loses its half power dependence on voltage, is independent of light intensity for the recombination limited case, whereas for the SCL photocurrent it scales with the square root of light intensity. In this study we investigate the origin of the low fill factor and photocurrent in low molecular weight PF10TBT:PCBM solar cells. A half power dependence of the photocurrent on voltage is observed and its origin is revealed by a combination of optical and electrical measurements and device simulations.

2. Experimental

PF10TBT was synthesized at the Netherlands Organisation for Applied Scientific Research (TNO) and used as received. In this study two batches were used, which will be identified by their weight average molecular weight (M_w) in the remainder of this paper. The low MW polymer had $M_w \sim 5.1 \times 10^3$ g/mol and polydispersity index PDI ~ 1.7, the high MW batch had $M_w \sim 1.9 \times 10^5$ g/mol and PDI ~ 3.5. The electron acceptor, PCBM, was obtained from Solenne. Polymer and fullerene were mixed in a 1:4 weight ratio and dissolved in chlorobenzene. Since the solubility of high MW PF10TBT in chlorobenzene at room temperature is low, solutions were stirred and processed at 90 °C. ITO-patterned glass substrates were cleaned, treated in a UV-ozone reactor and coated with a 40–60 nm thin hole-transporting buffer layer of PEDOT:PSS (H.C. Starck GmbH). The photoactive layer was spin coated in air with typically 80–100 nm thickness. Solar cells were finalized with evaporation of a 1 nm LiF/100 nm Al cathode to ensure an ohmic electron contact with the PCBM phase. To study hole transport properties of the blend, an electron-blocking 20 nm Pd/80 nm Au top contact was applied instead of the LiF/Al cathode.

Current–voltage characteristics were recorded using a Keithley 2400 SourceMeter. Measurements were performed in the dark and under illumination from an uncalibrated Steuernagel SolarConstant 1200 metal halide lamp with an estimated intensity equivalent to ca. 1.3 suns, as determined by comparison of measured and calculated short-circuit current densities (see below).

Spectral responsivity (SR) measurements were carried out with a lock-in amplifier, a transimpedance amplifier and a focused, chopped monochromatic beam from a quartz tungsten halogen lamp and several narrow band pass filters. An estimation of the short-circuit current density (J_{sc}) under standard test conditions was calculated by convolving the SR spectrum with the AM1.5G reference spectrum, using the verified premise of a linear dependence of J_{sc} on light intensity. The estimated illumination intensity for the material under study was taken as the ratio of the measured and calculated J_{sc}.

The refractive index n and extinction coefficient k of thin films of PF10TBT:PCBM were determined with variable-angle spectroscopic ellipsometry (VASE), using a VASE ellipsometer from J.A. Woollam Co., Inc. The VASE measurements were combined with transmission and reflection measurements to enable accurate fits of the experimental ellipsometric data in the employed wavelength range from 300 to 1500 nm. The optical constants of glass, ITO, quartz, silicon and PEDOT:PSS were determined first. For ITO and PEDOT:PSS, anisotropic optical constants were found. Since illumination during current–voltage measurements takes place at normal incidence, the components in the direction perpendicular to the plane of the substrate were used in the transfer-matrix calculations. The optical properties of LiF and aluminum were taken from literature. Next, the n and k of composite layers of PF10TBT and PCBM on various substrates were determined by fitting the data with several Gaussian oscillators. No

indications of anisotropy in the active layers were found and the data were interpreted with a uniform dielectric function throughout the layer.

3. Results and discussion

Fig. 1 shows the photovoltaic performance of equally thick PF10TBT:PCBM solar cells that were made using low (squares) and high (circles) molecular weight PF10TBT. The differences in fill factor and short-circuit current density are striking. Although both cells are 95 nm thick, the high MW cell produces a 30% higher J_{sc} compared to its low MW counterpart. The fill factor increases significantly with molecular weight as well: it improves from 0.45 to 0.63. In the remainder of this article, we will systematically address the importance of the various effects of a change in molecular weight on device performance.

First, considering the marked difference in J_{sc}, one might anticipate a change in absorption due to variations in, for example, interchain interactions [12,17]. Usually low MW polymers exhibit a blue-shift in solid-state absorption. In a photovoltaic cell this may alter the number of photogenerated excitons and therefore the magnitude of the photocurrent, depending on the overlap of the absorption profile with the irradiance spectrum. When the absorption maximum changes in magnitude as well, the effect of changing MW on J_{sc} may be intensified. Fig. 2 shows the refractive index n and extinction coefficient k of composite layers of PF10TBT and PCBM, as determined with variable-angle spectroscopic ellipsometry. In the region where PF10TBT contributes most to the absorption of the blend layer, i.e., between 450 and 650 nm, the extinction coefficient of the low MW sample (black solid line) is indeed blue-shifted. In addition, the magnitude of k in this region is much lower. Due to optical interference effects, which play an important role in thin films capped with a highly reflective aluminum cathode [18], it is expected that the extent to which a change in optical constants influences the absorption in the active layer varies with the thickness of the layer. The consequences of reduced absorption in low MW solar cells can be quantified by modeling of the optical electric field inside the device [18–20]. Using the transfer-matrix approach described by Pettersson et al. in Ref. [18], provided with the optical constants of Fig. 2 and the AM1.5G solar irradiance spectrum, we calculated the amount of photons that are absorbed each second in the bulk of the active layer as a function of position in the device, for both MW cases. The results are shown in Fig. 3. The active layer in the low MW device clearly absorbs less photons due to its lower extinction coefficient, yet the difference between the profiles is not as large as one might expect from consideration of the optical constants. Integration of the photon absorption rates over the position gives total photon absorption rates of $4.8 \times 10^{20}\ m^{-2}\ s^{-1}$ and $5.1 \times 10^{20}\ m^{-2}\ s^{-1}$ for low and high MW, respectively. Since these cells show a linear dependence of J_{sc} on light intensity, the observed difference of 30% in short-circuit current density cannot be explained by this increase of

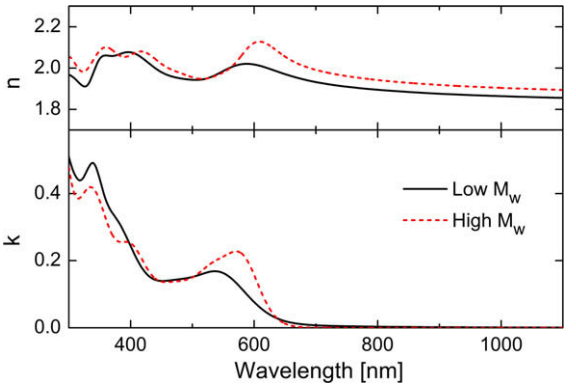

Fig. 2. Index of refraction n and extinction coefficient k of PF10TBT:PCBM layers on glass. The heterojunction from the low MW polymer (solid line) shows reduced absorption compared to the one containing high MW PF10TBT (dotted line). (For interpretation of the references to colour in this figure legend, the reader is referred to the web version of this article.)

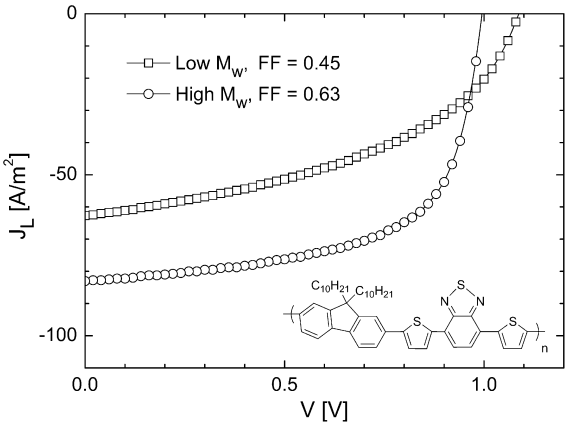

Fig. 1. Current density under illumination (J_L) versus voltage characteristics of PF10TBT:PCBM solar cells made from low (squares) and high (circles) molecular weight PF10TBT. Both active layers were approximately 95 nm thick. The inset shows the chemical structure of PF10TBT.

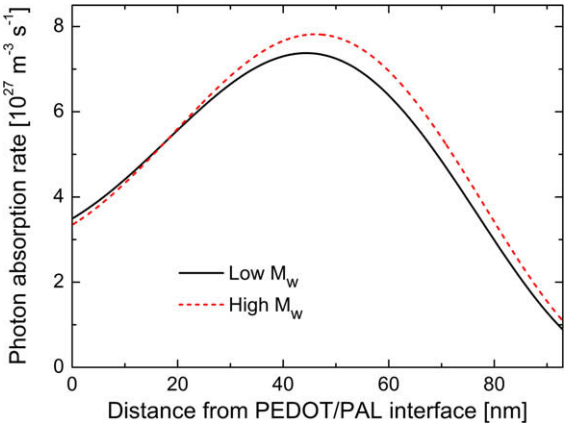

Fig. 3. Photon absorption profiles calculated for the devices of Fig. 1, using the optical constants presented in Fig. 2. (For interpretation of the references to colour in this figure legend, the reader is referred to the web version of this article.)

6% in absorption only. Furthermore, no significant influence on the fill factor would be expected. We therefore conclude that optics only account for a minor part of the variation in photovoltaic performance.

Other than optical effects, a change of molecular weight might cause electronic differences. As stated in the introduction, space-charge effects can limit the fill factor of an organic solar cell to 0.42. Such a limitation can only occur if charge transport in the solar cell is strongly unbalanced. A significant effect of polymer molecular weight on the electron mobility in the PCBM phase is highly unlikely, since the acceptor constitutes the largest part (80 wt.%) of the active layer. The electron mobility μ_e can be probed by consideration of the current through the solar cells in the dark. In fullerene-based solar cells, the dark current under forward bias is usually dominated by electrons due to their high mobility in the PCBM phase. As shown in Fig. 4, the dark current of the PF10TBT:PCBM solar cells under study is well described by the single carrier space-charge limited current (SCLC) [21],

$$J = \frac{9}{8}\varepsilon_0\varepsilon_r\mu_e\frac{V^2}{L^3} \tag{2}$$

with L the layer thickness, $\mu_e = 8 \times 10^{-8}$ m^2/Vs for low MW PF10TBT and $\mu_e = 1 \times 10^{-7}$ m^2/Vs for the high MW case. The applied voltage was corrected for the built-in voltage (V_{bi}) and resistive losses in the ITO/PEDOT anode (V_{Rs}). The relative dielectric constant ε_r was taken as the spatial average of PF10TBT and PCBM. As expected, the electron mobility is hardly affected by the molecular weight of the polymer and its value is close to what has been found previously for PCBM in fullerene-based solar cells [22–24]. Limitations to the photocurrent, if any, should therefore be caused by a low hole mobility in the low MW polymer. To elucidate the influence of molecular weight on hole transport in PF10TBT based solar cells, we prepared hole-only diodes from PF10TBT:PCBM bulk heterojunctions in a 1:4 weight ratio. The current density versus effective voltage characteristics presented in Fig. 5 were measured at room temperature for two such devices using low MW (squares) and high MW (circles) PF10TBT. The single carrier space-charge limited currents were modeled using exactly the same low-field hole mobility of 6×10^{-9} m^2/Vs (solid lines). Hence, no effect of molecular weight on the mobility in the PF10TBT phase was found. Measurements on pristine polymer layers revealed similar mobility values in both MW cases, showing that the hole transport in the PF10TBT:PCBM blend is also not affected by PCBM loading. This behavior contrasts to the case of MDMO-PPV:PCBM heterojunctions [23,25] and to what has been reported for a similar polyfluorene copolymer [26]. From temperature-dependent measurements, the thermal activation energy of hole transport in the blend was found to be 0.33 eV in both cases. This exactly equals the theoretically predicted value, obtained from the relation between the universal mobility prefactor $\mu_0 = 3 \times 10^{-3}$ m^2/Vs and the above-mentioned low-field mobility at room temperature [27]. Since the hole mobility in the blend is constant with molecular weight, and differs only an order of magnitude with the electron mobility in PCBM, a space-charge limitation of the photocurrent in these relatively thin solar cells is highly unlikely [28].

Fig. 6 presents a comparison of the photocurrent of two cells based on low (squares) and high (circles) molecular weight PF10TBT, plotted versus effective voltage. Here, the experimental photocurrent is defined as the difference between the current density under illumination J_L and in the dark J_D, thus $J_{ph} = J_L - J_D$. Since the photocurrent is zero at $V = V_0$, the horizontal axis represents the effective voltage available for charge extraction from the device. In both cases the photocurrent nicely saturates at high effective voltage, indicating that at sufficiently large reverse bias all photogenerated bound pairs are dissociated and

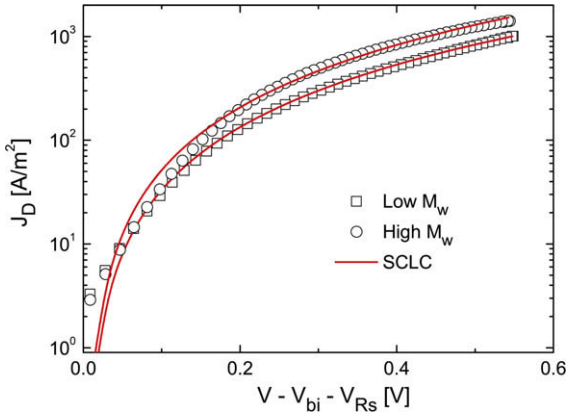

Fig. 4. Determination of the electron mobility from the dark current of PF10TBT:PCBM solar cells (symbols) using the single carrier SCLC (solid lines). The fits reveal an electron mobility in PCBM of $\mu_e = 8 \times 10^{-8}$ m^2/Vs for low MW PF10TBT and $\mu_e = 1 \times 10^{-7}$ m^2/Vs for the high MW case. The applied voltage was corrected for the built-in voltage (V_{bi}) and the voltage loss over the ITO/PEDOT anode (V_{Rs}). (For interpretation of the references to colour in this figure legend, the reader is referred to the web version of this article.)

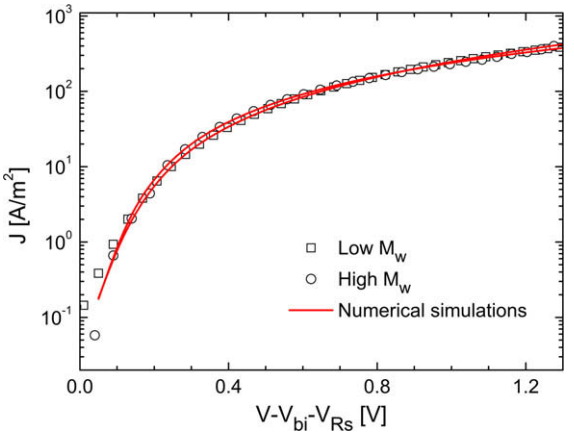

Fig. 5. Current–voltage data of hole-only diodes of bulk heterojunctions containing low (squares) and high (circles) MW PF10TBT. The solid lines represent numerical simulations, both using a low-field hole mobility of $\mu_h = 6 \times 10^{-9}$ m^2/Vs. The applied voltage was corrected for the built-in voltage (V_{bi}) and the voltage loss over the ITO/PEDOT anode (V_{Rs}). (For interpretation of the references to colour in this figure legend, the reader is referred to the web version of this article.)

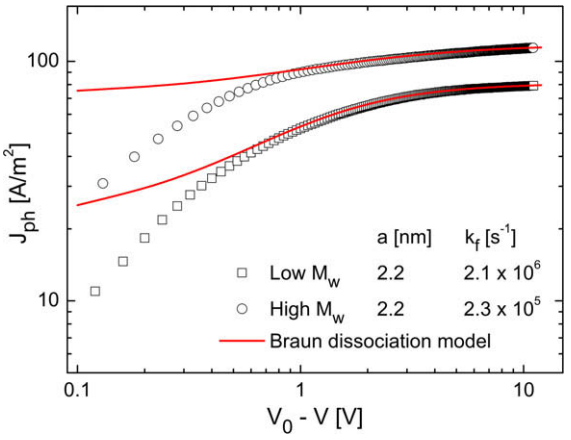

Fig. 6. Experimental photocurrents in solar cells from low (squares) and high (circles) molecular weight PF10TBT. The lines denote calculations of $J_{ph} = qGL$, using a field and temperature-dependent generation rate $G(T,E) = G_{max}P(T,E)$ as given by Braun's model of dissociation of charge transfer states [30]. (For interpretation of the references to colour in this figure legend, the reader is referred to the web version of this article.)

extracted from the device. The occurrence of saturation was verified with temperature-dependent measurements (not shown). At lower voltages, however, the photocurrent of the low MW cell clearly depends stronger on the electric field as compared to the high MW cell. In this voltage regime, a square root dependence is observed. This is indicated by the tilted dotted lines with slope ½ in Fig. 7, which shows intensity dependence measurements of the photocurrent in the low MW solar cell. The experimental photocurrent depends linearly on light intensity and the saturation voltage V_{sat} is intensity independent. This combination of voltage and intensity dependence of the photocurrent is a clear fingerprint of a recombination limited photocurrent.

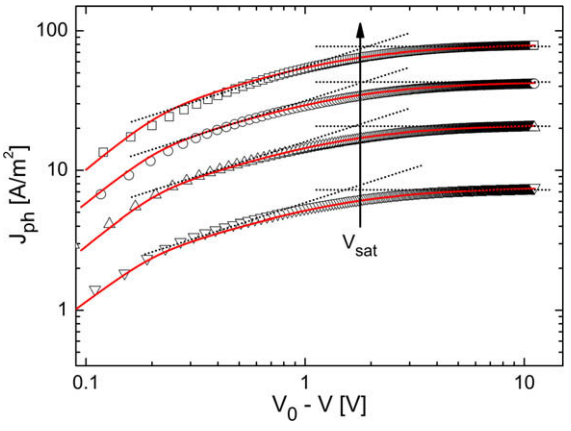

Fig. 7. Intensity dependent photocurrent of the same low MW device as shown in Fig. 6. The tilted dotted lines denote slope ½, indicating $J_{ph} \propto V^{0.5}$, whereas the horizontal dotted lines mark the saturated photocurrent at each intensity. The solid lines represent numerical device simulations. (For interpretation of the references to colour in this figure legend, the reader is referred to the web version of this article.)

Application of Eq. (1) in the square root regime reveals a free carrier lifetime of approximately 0.5 μs. However, as was mentioned before, illumination of organic solar cells does not directly result in free charge carriers: instead, after charge transfer a bound electron–hole pair is created. Due to the high Coulomb binding energy in organic solar cells, only a certain fraction of all photogenerated bound electron–hole pairs G_{max} is dissociated into free charge carriers, depending on field and temperature, and therefore contributes to the photocurrent $J_{ph} = qGL$. Consequently, the generation rate G of free charge carriers can be described by:

$$G(T,E) = G_{max}P(T,E) \tag{3}$$

where $P(T,E)$ is the probability for charge separation at the donor/acceptor interface. The photogeneration of free charge carriers in low-mobility materials can be explained by the geminate recombination theory of Onsager [29]. An important addition to the theory has been made by Braun [30], who stressed the importance of the fact that the bound electron–hole pair (or charge transfer state) has a finite lifetime. In Braun's model, the probability that a bound polaron pair dissociates into free charge carries at a given electric field E and temperature T is given by:

$$P(T,E) = \frac{k_{diss}(E)}{k_{diss}(E) + k_f} \tag{4}$$

with k_f the rate constant with which the bound electron–hole pair decays to its ground state, and $k_{diss}(E)$ the rate constant for separation into free carriers, which is given by [30]:

$$k_{diss}(E) = \frac{3k_R}{4\pi a^3} e^{-E_B/k_BT}\left[1 + b + \frac{b^2}{3} + \frac{b^3}{18} + \frac{b^4}{180} + \cdots\right] \tag{5}$$

with a the initial separation distance of the bound electron–hole pair at the interface, $b = e^3E/8\pi\varepsilon_0\varepsilon_r k_B{}^2T^2$, and E_B the binding energy of the electron–hole pair.

Once separated, the charge carriers can again form a bound pair with rate constant k_R. The dissociation model uses Onsager theory for field-dependent dissociation rate constants for weak electrolytes [29] for $k_{diss}(E)$, Langevin recombination of free electrons and holes [31] and a Gaussian distribution of donor–acceptor distances. Then, the generation rate of free electrons and holes depends on the charge carrier mobilities μ_e and μ_h of the electrons and holes respectively, the relative dielectric constant ε_r, the initial separation of e–h pairs a, and the ground state recombination rate k_f.

As expressed in Eq. (4), the relative magnitudes of dissociation and decay rates determine a field and temperature-dependent dissociation probability of bound pairs $P(T,E)$. Consequently, when the photocurrent of an organic solar cell is interpreted using Eq. (1), the obtained lifetime is in fact an *effective* lifetime, equal to $P(T,E)\tau$, where τ is now the true lifetime of free charge carriers [16]. Using device modeling, we can determine whether a low effective lifetime originates from short lifetimes of bound pairs (low P) or free carriers (low τ).

We continue the investigation of the molecular weight dependent photocurrents in Fig. 6 by modeling the field-

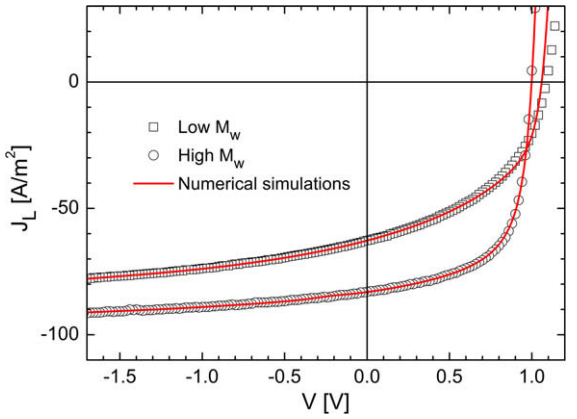

Fig. 8. Experimental (symbols) and simulated (lines) current–voltage characteristics of the solar cells of Fig. 1 under illumination. The lines show numerical fits that only differ in the used values of G_{max} (representing enhanced absorption in high MW PF10TBT) and k_f (obtained from Fig. 6). (For interpretation of the references to colour in this figure legend, the reader is referred to the web version of this article.)

dependent generation. The solid lines represent calculations of the photocurrent according to $J_{ph} = qGL$, using a field and temperature-dependent generation rate of free carriers as given by Braun's model [30,32]. The dissociation probability $P(T,E)$ is parameterized by the initial separation distance of the bound electron–hole pair a and the decay rate k_f, which are now the only fit parameters since L is measured separately and G_{max} can be calculated directly from $J_{ph} = qG_{max}L$ in the saturation regime. The fits reveal a value of $a = 2.2$ nm, irrespective of molecular weight. However, the decay rate k_f in the low MW cell is at $2.1 \times 10^6\ s^{-1}$ an order of magnitude higher than k_f of the high MW cell. This value of k_f is in very good agreement with the effective lifetime of free carriers as determined from Eq. (1), since $(0.5\ \mu s)^{-1} = 2 \times 10^6\ s^{-1}$.

To model the photocurrent over the entire effective voltage range, we utilized our numerical device model [33]. Since diffusion of charge carriers is now also taken into account, the photocurrent can be simulated at low effective voltage as well. In the simulations, shown in Fig. 7, the experimentally determined values of the charge carrier mobilities, layer thickness, dissociation parameters a and k_f, and generation rate of bound pairs G_{max} were used. The calculations excellently fit the measured data at various light intensities. This clearly shows that the photocurrent of low molecular weight PF10TBT:PCBM cells is limited by recombination of short-lived bound electron–hole pairs. We speculate that the limitation arises from insufficient phase separation, resulting in localization of bound pairs in isolated donor–acceptor regions, which prohibits efficient dissociation. Indeed, transmission electron microscopy (TEM) measurements on blends of varying molecular weight have revealed little contrast in blends of low MW PF10TBT with PCBM, whereas pronounced PCBM and polymer rich regions were observed in high MW films [8].

Fig. 8 presents a direct comparison of the simulated current–voltage characteristics under illumination of the cells

Table 1
Parameters used to fit the current–voltage characteristics presented in Fig. 8.

Parameter	Symbol	Value	
		Low MW	High MW
Band gap	E_{gap}	1.47 eV	1.38 eV
Electron mobility	μ_e	$8 \times 10^{-8}\ m^2/Vs$	$1 \times 10^{-7}\ m^2/Vs$
Hole mobility	μ_h	$6 \times 10^{-9}\ m^2/Vs$	$6 \times 10^{-9}\ m^2/Vs$
Eff. density of states	N_c	$2.5 \times 10^{25}\ m^{-3}$	$2.5 \times 10^{25}\ m^{-3}$
Generation rate	G_{max}	$6.0 \times 10^{27}\ m^{-3}\ s^{-1}$	$6.6 \times 10^{27}\ m^{-3}\ s^{-1}$
Rel. dielectric constant	ε_r	3.6	3.6
Initial e/h pair distance	a	2.2 nm	2.2 nm
e/h Pair decay rate	k_f	$2.1 \times 10^6\ s^{-1}$	$2.3 \times 10^5\ s^{-1}$

of Fig. 1. The model parameters that were used to fit the current–voltage curves are summarized in Table 1. Compared with the simulation of the curve of the low MW cell, only three input parameters were changed to fit that of the high MW cell: the slightly higher, experimentally determined electron mobility was used, G_{max} was increased by 10% and the previously determined lower decay rate $k_f = 2.3 \times 10^5\ s^{-1}$ was used. The increase in G_{max} closely agrees with the small (6%) enhancement in the calculated absorption for high MW cells as presented in Fig. 3. For these relatively thin active layers, using a constant generation rate G_{max} throughout the active layer does not change the simulation results compared to the use of the calculated optical profile as input [34]. The slightly higher V_{oc} of the low MW cell originates from the inversely proportional relationship between the polymer band gap and the average number of repeating units in each chain [35]. At short-circuit conditions, the average dissociation probability of bound electron–hole pairs in the high MW cell is 19% higher (relative) than in the low MW device, due to the reduction in k_f. Thus, the concomitant effects of enhanced absorption (10%) and more efficient dissociation (19%) add up to the observed increase of short-circuit current (30%) and fill factor.

4. Conclusions

Using optical and electronic device modeling, we have unraveled the molecular weight dependence of the short-circuit current density and fill factor of PF10TBT:PCBM solar cells. The use of high molecular weight PF10TBT causes an enhancement of the extinction coefficient of the blend layer, resulting in a slight increase in the amount of photons that are absorbed. Charge transport in both phases was found to be virtually unaffected by a change in molecular weight. The electron mobility in the blend is only slightly higher for high MW PF10TBT and a reasonably high, molecular weight independent hole mobility was measured in blend layers as well as pristine polymer layers, which renders the influence of space-charge on the photocurrent insignificant. Intensity dependence measurements confirmed that the photocurrent of low molecular weight cells is recombination limited. From numerical device simulations, we conclude that a low dissociation prob-

ability of short-lived bound electron–hole pairs is the main cause of the poor performance. The limitation is most likely caused by insufficient phase separation, which leads to localization of charges on isolated parts of the donor and acceptor phases.

Acknowledgements

This work was funded by SenterNovem via the EOS Long Term program ZOMER (EOS LT 03026). This work was partly supported by the Dutch Polymer Institute (DPI), Project DPI No. 524.

References

[1] G. Yu, J. Gao, J.C. Hummelen, F. Wudl, A.J. Heeger, Science 270 (1995) 1789.
[2] M.A. Green, K. Emery, Y. Hishikawa, W. Warta, Prog. Photovoltaics Res. Appl. 17 (2009) 85.
[3] M. Svensson, F. Zhang, S.C. Veenstra, W.J.H. Verhees, J.C. Hummelen, J.M. Kroon, O. Inganäs, M.R. Andersson, Adv. Mater. 15 (2003) 988.
[4] O. Inganäs, M. Svensson, F. Zhang, A. Gadisa, N.K. Persson, X. Wang, M.R. Andersson, Appl. Phys. A 79 (2004) 31.
[5] T. Yohannes, F. Zhang, M. Svensson, J.C. Hummelen, M.R. Andersson, O. Inganäs, Thin Solid Films 449 (2004) 152.
[6] L.H. Slooff, S.C. Veenstra, J.M. Kroon, D.J.D. Moet, J. Sweelssen, M.M. Koetse, Appl. Phys. Lett. 90 (2007) 143506.
[7] D.J.D. Moet, L.H. Slooff, J.M. Kroon, S.S. Chevtchenko, J. Loos, M.M. Koetse, J. Sweelssen, S.C. Veenstra, in: Proceedings of the MRS Fall Meeting, Warrendale, PA, Boston, 2007, pp. CC03–CC09.
[8] S.C. Veenstra, D.J.D. Moet, J. Sweelssen, S.S. van Bavel, E. Voroshazi, M.M. Koetse, J. Loos, B. de Boer, P.W.M. Blom, J.M. Kroon, Polyfluorene:[C60]PCBM Based Solar Cells; A Correlation Between the Molecular Weight of the Polymer and the Photovoltaic Performance, Presented at the E-MRS 2009 Spring Meeting, Strasbourg, France, 2009.
[9] V.D. Mihailetchi, J. Wildeman, P.W.M. Blom, Phys. Rev. Lett. 94 (2005) 126602.
[10] R.J. Kline, M.D. McGehee, E.N. Kadnikova, J. Liu, J.M.J. Fréchet, Adv. Mater. 15 (2003) 1519.
[11] R.J. Kline, M.D. McGehee, E.N. Kadnikova, J. Liu, J.M.J. Frechet, M.F. Toney, Macromolecules 38 (2005) 3312.
[12] A. Zen, J. Pflaum, S. Hirschmann, W. Zhuang, F. Jaiser, U. Asawapirom, J.P. Rabe, U. Scherf, D. Neher, Adv. Funct. Mater. 14 (2004) 757.
[13] C. Goh, R.J. Kline, M.D. McGehee, E.N. Kadnikova, J.M.J. Frechet, Appl. Phys. Lett. 86 (2005) 122110.
[14] A.M. Ballantyne, L. Chen, J. Dane, T. Hammant, F.M. Braun, M. Heeney, W. Duffy, I. McCulloch, D.D.C. Bradley, J. Nelson, Adv. Funct. Mater. 18 (2008) 2373.
[15] A.M. Goodman, A. Rose, J. Appl. Phys. 42 (1971) 2823.
[16] M. Lenes, M. Morana, C.J. Brabec, P.W.M. Blom, Adv. Funct. Mater. 19 (2009) 1106.
[17] J.-F. Chang, J. Clark, N. Zhao, H. Sirringhaus, D.W. Breiby, J.W. Andreasen, M.M. Nielsen, M. Giles, M. Heeney, I. McCulloch, Phys. Rev. B 74 (2006) 115318.
[18] L.A.A. Pettersson, L.S. Roman, O. Inganas, J. Appl. Phys. 86 (1999) 487.
[19] Z. Knittl, Optics of Thin Films, John Wiley and Sons, 1976.
[20] H. Hoppe, N. Arnold, N.S. Sariciftci, D. Meissner, Sol. Energy Mater. Sol. Cells 80 (2003) 105.
[21] M.A. Lampert, P. Mark, Current Injection in Solids, Academic Press, New York, 1970.
[22] V.D. Mihailetchi, J.K.J. van Duren, P.W.M. Blom, J.C. Hummelen, R.A.J. Janssen, J.M. Kroon, M.T. Rispens, W.J.H. Verhees, M.M. Wienk, Adv. Funct. Mater. 13 (2003) 43.
[23] V.D. Mihailetchi, L.J.A. Koster, P.W.M. Blom, C. Melzer, B. de Boer, J.K.J. van Duren, R.A.J. Janssen, Adv. Funct. Mater. 15 (2005) 795.
[24] V.D. Mihailetchi, H.X. Xie, B. de Boer, L.J.A. Koster, P.W.M. Blom, Adv. Funct. Mater. 16 (2006) 699.
[25] C. Melzer, E.J. Koop, V.D. Mihailetchi, P.W.M. Blom, Adv. Funct. Mater. 14 (2004) 865.
[26] K.G. Jespersen, F. Zhang, A. Gadisa, V. Sundström, A. Yartsev, O. Inganäs, Org. Electron. 7 (2006) 235.
[27] N.I. Craciun, J. Wildeman, P.W.M. Blom, Phys. Rev. Lett. 100 (2008) 056601.
[28] M. Lenes, L.J.A. Koster, V.D. Mihailetchi, P.W.M. Blom, Appl. Phys. Lett. 88 (2006) 243502.
[29] L. Onsager, J. Chem. Phys. 2 (1934) 599.
[30] C.L. Braun, J. Chem. Phys. 80 (1984) 4157.
[31] L.J.A. Koster, V.D. Mihailetchi, P.W.M. Blom, Appl. Phys. Lett. 88 (2006) 052104.
[32] V.D. Mihailetchi, L.J.A. Koster, J.C. Hummelen, P.W.M. Blom, Phys. Rev. Lett. 93 (2004) 216601.
[33] L.J.A. Koster, E.C.P. Smits, V.D. Mihailetchi, P.W.M. Blom, Phys. Rev. B 72 (2005) 085205.
[34] J.D. Kotlarski, P.W.M. Blom, L.J.A. Koster, M. Lenes, L.H. Slooff, J. Appl. Phys. 103 (2008) 084502.
[35] R. Hoffmann, C. Janiak, C. Kollmar, Macromolecules 24 (1991) 3725.